Experimental demonstration of fiber Bragg grating strain sensors for structural vibration control

4 AUTHORS, INCLUDING:

Kelvin Chau
University of California, San Diego
17 PUBLICATIONS **119** CITATIONS

SEE PROFILE

B. Moslehi
Intelligent Fiber Optic Systems (IFOS) Corpor…
76 PUBLICATIONS **1,259** CITATIONS

SEE PROFILE

Experimental Demonstration of Fiber Bragg Grating Strain Sensors for Structural Vibration Control

K. Chau[a] and B. Moslehi[a], G. Song[b] and V. Sethi[b]

[a]Intelligent Fiber Optics System Corporation (IFOS), 650 Vaqueros Avenue, Sunnyvale, CA 94085
www.ifos.com
[b]Department of Mechanical Engineering, University of Houston, Houston TX 77204

ABSTRACT

We report on the use of a high-speed wavelength division multiplexing (WDM) technique for multiplexing Fiber Bragg Grating (FBG) sensors applied to structural Vibration Control for the measurement of strain, permitting many sensing devices along a single optical fiber at different locations collecting samples at 5000 Hz with microstrain resolution. In this demonstration, a cantilevered flexible aluminum beam is used as the object for vibration control. A piezoceramic patch surface-bonded to the cantilevered end of the beam is used as an actuator to suppress the beam vibration. Various active vibration controllers such as positive position feedback (PPF), strain rate feedback (SRF), proportional plus derivative (PD), pole placement, and sliding mode based robust control are tested by using the fiber optical sensor for feedback purpose. Experiments successfully demonstrate that the signals from the fiber optic sensor can be used for active feedback control of the beam vibration.

Key words: active vibration control, fiber optic sensors, positive position feedback control, strain rate feedback control, piezoelectric materials.

1. INTRODUCTION

Optical fiber sensors were introduced over a decade ago for vibration sensing and monitoring. Huston *et al.* 1991[1] presented results of using a statistical-mode fiber optic sensor as a spatially distributed vibration transducer for monitoring the vibrations of a structural member on a scaled laboratory bridge model. The fiber optic vibration measurements were compared with simultaneous piezoelectric accelerometer point measurements. Berkoff *et al.* 1994[2] described the use of Fiber Bragg Grating (FBG) sensors for distributed vibration sensing and monitoring.

FBGs are used extensively in the telecommunication industry for Dense Wavelength Division Multiplexing (DWDM), laser stabilization, and optical amplifier gain flattening. Optical fiber sensors based on FBGs have also been demonstrated successfully in oil & gas, civil, aeronautical and mechanical engineering applications such as aircraft and civil structuring health monitoring. FBG sensors embedded throughout the body of bridge and aircraft can monitor structural stress, providing improved accuracy, resolution and sensitivity over existing systems. This type of sensor is rugged, lightweight and immune to electromagnetic interference, can be multiplexed based on wavelength and/or time division multiplexing techniques, and can monitor several locations distributed over long distances using a single light source, detector and signal processing system, allowing configurations with all the electronics at a location remote from the monitored region.

FBG sensors are commonly fabricated by writing an index grating directly on a doped optical fiber, forming an interference pattern with the desired periodicity. The FBG wavelength filter consists of a series of perturbations in the index of refraction along the length of the doped optical fiber. The physical principle behind FBG sensors is that a change in strain, stress, or temperature will alter the center of the wavelength of the light reflected from an FBG. This index grating reflects a narrow spectrum whose center wavelength that is directly proportional to the period of the index modulation (Λ) and the effective index of refraction (n). More specifically, the wavelength at which the

reflectivity peaks, referred to as the Bragg wavelength (λ_B), is given by $\lambda_B = 2 n\Lambda$. Because temperature and strain directly affect Λ and n, any change in temperature and strain directly affects λ_B. In the 1550-nm (C-Band) window, the main telecommunications transmission frequency, a change in mechanical or thermal strain on the FBG written in fused silica fiber results in a wavelength/strain sensitivity of approximately 1.2 pm/μstrain (one microstrain corresponds to a change in dimension of one part per million) and a wavelength/temperature sensitivity of 10 pm/°C. The gauge lengths of FBGs are typically up to 5 mm, although lengths of up to 100 cm are being developed for civil-engineering applications.

Optical fiber sensors have also been used in the control of smart structures applications. Lindner *et al.* 1990[3] discussed the performance of a velocity feedback control system for vibration suppression in a flexible beam using a modal domain fiber-optic sensor. Cox and Lindner 1991[4] demonstrated the applications of fiber optic sensors in active control. Juang and Wu 1995[5] also presented active control of cantilever beam structure using fiber interferometric sensor. Chien *et al.* 1996[6] used fiber optics Michelson interferometric sensor to detect the vibration signal in a flexible beam and then implemented the active control technique to suppress the vibrations using the piezoelectric transducer. Serdar *et al.* 1997[7] discussed active vibration control technique using embedded or bonded piezoelectric actuators and multi- channel fiber-optics sensors. They implemented the time-delay technique for active vibration control and compared its performance over other conventional control techniques.

Vibration control[8] is a field of increasing and wide-ranging importance for noise reduction, safety enhancement and structural longevity as well as precision manufacturing. For example: (1) noise suppression in automobile, aircraft and industrial engines will be universally appreciated; (2) in spacecraft, vibration control has the potential for (a) weight minimization while ensuring stability of structural components, (b) protection of expensive, fragile payloads, (c) allowing release into their orbits as accurately as possible; (3) noise and vibration control is particularly useful where critical listening, conferencing or living spaces are located adjacent to noise or vibration sources.

In this paper, we report on application of an FBG sensing system to structural vibration control. Experiments were conducted on cantilevered beam for active vibration control using the signals sampled at 5 kHz with microstrain resolution from the fiber optic sensor. To experimentally demonstrate the effectiveness of using an FBG system for structural vibration control, four active vibration control methods were implemented. Piezoelectric transducers were used as actuators for the excitation of the flexible beam and as well as for the control action. Discussion on use piezoelectric transducers in intelligent structures can be found in papers by Crawley 1987[9], 1988[10], 1994[11]. The active control techniques for the present research include pole placement control, positive position feedback (PPF), strain rate feedback (SRF) and sliding mode control. Pole placement control has been used in small flexible beams by Manning *et al.* 2000[12] and Bu *et al.* 2003[13] wherein they used parameter identification technique by identifying the ARMAX model and then implemented the designed controller. Scott *et al.* 2001[14] also used the pole placement control for flexible beams. Positive position feedback (PPF) (Goh and Caughey, 1985[15], Fanson and Caughey 1990[16]; Agrawal and Bang, 1994[17]; Baz and Poh 1996[18], Friswell and Inman 1999[19], and Song *et al.*, 2000[20]) is applied by feeding the structural position coordinate directly to the compensator, and the product of the compensator and a scalar gain positively back to the structure. PPF offers quick damping for a particular mode provided that the modal characteristics are known. PPF is also easy to implement. Song *et al.* (1998)[20] experimentally demonstrated that PPF is robust to a varying modal frequency. Strain Rate Feedback (SRF) control is used for active damping of a flexible space structure (Newman, 1992[22]). Using SRF, the structural velocity coordinate is fed back to the compensator and the compensator position coordinate multiplied by a negative gain is fed back to the structure. SRF has a wider active damping region and can stabilize more than one mode given a sufficient bandwidth. Experimental results successfully demonstrated that the pole placement control, PPF, SRF and sliding mode control methods are effective in actively increasing damping of the flexible beam with PZT actuators and fiber Bragg grating sensors.

2. FIBER BRAGG GRATING SENSING SYSTEM

A variety of different techniques had been developed for interrogating the FBG sensors while permitting the multiplexing of many of these devices along a single optical fiber.[23-26] The system used to provide measurements in the experiment was from Intelligent Fiber Optic System (IFOS)[29-30]. Shown in Figure 1 is the basic operation

principle and configuration of the system to support an array of FBG sensors simultaneously. A 1550-nm broadband source of approximately 1 mW power and 30 nm spectral width was used to illuminate a string of gratings with Bragg wavelengths λ_{Bn} through a 3-port optical circulator. The signals returned from the FBG sensors were dropped at the third port of circulator and processed through proprietary optical signal processing circuitry providing wavelength separation and high-speed wavelength measurement. Parallel processing enables the system to interrogate multiple FBG sensors simultaneously at high speed. The particular system shown in Fig. 1 is capable of interrogating four FBG sensors simultaneously at 5 kHz. However, additional sensors can be accommodated[30].

Dynamic strain can be measured by noting that the wavelengths reflected from each FBG shift dependent on the strain applied to that FBG. In particular, when an FBG changes length (i.e., is stretched or compressed) its reflected wavelength λ_{Bn} changes by an amount $\delta\lambda_{Bn}$ in linear proportion to the strain ε imposed onto the fiber according to the relation:

$$\delta\lambda_{Bn}/ \varepsilon \approx \lambda_{Bn} (1 - p_e) \approx (\lambda_{Bn} /1550 \text{ nm}) \, 1.21 \text{ pm / microstrain} \tag{1}$$

where $p_e \approx 0.22$ is the photoelastic coefficient for silica.

In this demonstration, a cantilevered flexible aluminum beam was used as the object for vibration control and a piezo-ceramic patch surface-bonded to the cantilevered end of the beam used as an actuator to suppress the beam vibration. An FBG sensor was mounted to the beam, where the maximum strain was detected. The FBG sensor was connected via standard single mode fiber to the interrogation system that performed the reflected wavelength measurement as described above. The system converted the strain-dependent optical wavelength reflected from each sensor into a pair of analog, DC-coupled signals, one being the reference voltage dependent on the optical power; another the voltage related to wavelength shift. These signals were real-time readouts and used as the direct feedback to the software as part of closed loop control.
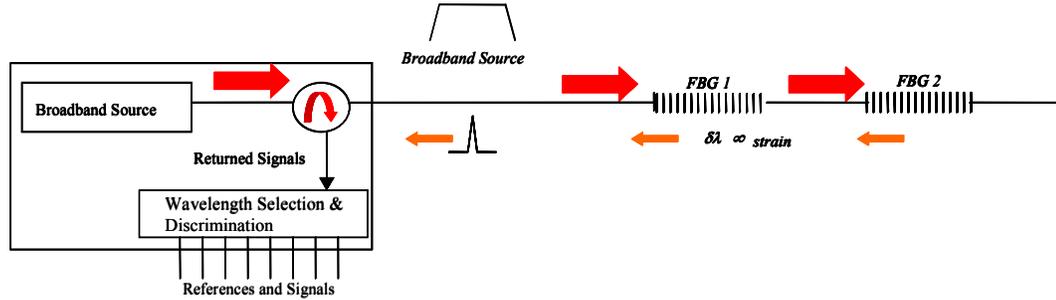

Fig. 1 Basic operation principle and configuration of Interrogation System

3. EXPERIMENTAL SETUP

The objective is to show the effectiveness of using FBG sensing system for various feedback vibration suppression strategies for a flexible beam. To achieve this control objective an experiment is set up. The flexible beam used in this experiment is made of aluminum and its properties are listed in Table 1. Figure 2 shows the experimental set up of the beam in a cantilevered configuration. The beam has very low damping characteristics and exhibits significant vibrations when excited.

Two piezoceramics patches of lead zirconate titanate (PZT) QP 10W are surface bonded at the cantilevered end of the beam for the purpose of actuation of the beam. The PZT QP 10 W is product from ACX Incorporation. The property of PZT QP10 W is shown in Table 2. In this experiment, there is one input for the 2 actuators and 1 output was recorded from the fiber Bragg grating sensor. A phase shifter was needed in this implementation to amplify the signal from the sensors and also to eliminate the high frequency noise content from the sensor signal. For implementing the controller in real time, a dSPACE digital data acquisition and real-time control system is used.

The dSPACE uses a DS1103 digital signal process board for real-time control implementations. The dSPACE system also has integrated analog-to-digital and digital-to-analog converters.

Fig. 2 Experimental Set-up

Table 1. Beam Properties

Symbol	Quantity	Units	Value
L	Beam Length	mm	736.5
w_b	Beam width	mm	53.1
t_b	Beam thickness	mm	1
ρ_b	Beam density	kg/m^3	2690
E	Modulus of elasticity	N/m^2	7.03×10^{10}

Table 2. PZT Patch Properties

Symbol	Quantity	Units	PZT ACTUATOR
$L \times w \times t$	Dimensions	mm	$46 \times 33.27 \times 0.25$
d_{33}	Strain coefficient	C/N	7.41×10^{-10}
d_{31}	Strain coefficient	C/N	-2.74×10^{-10}
ρ_p	PZT density	kg/m^3	7500
E_p	Young's Modulus	N/m^2	6.3×10^{10}

4. VIBRATION SUPPRESSION METHODS

To demonstrate the effectiveness of using fiber optics Bragg gratings as sensors for active vibration control various control strategies including linear and non-linear control are applied. In this paper, four vibration-suppression methods were used viz. pole placement control, positive position feedback, strain rate feedback and sliding mode control. The basic theory governing these methods is given below.

3.1 Pole Placement Control

Pole placement control offers the flexibility to the designer to relocate the poles of the system so as to achieve desired performance of the system. State space approach offers the designer to select n independent gains in a system so that the arbitrarily assigned/desired poles performance is achieved. In our problem of vibration suppression, the requirement is to increase the damping of the system in order to quell the excessive vibrations. To analyze the above problem the first step was to model the system. A second order system which depicts the single degree of freedom of frequency at 1.64 Hz was identified for the flexible beam. Log decrement was used to experimentally identify the damping associated with the frequency at 1.64 Hz. This system was used in the state space approach to find the feedback gains by the Ackerman method and to place the poles at such a location so as to increase the damping. The following state space matrices represent the above system.

$$\dot{x} = Ax + Bu$$
$$y = Cx$$
(2)

The state feedback gain matrix G obtained by the feedback law,

$$u = -Gx$$
(3)

in a system is selected to achieve the performance of the closed loop system. In this case the desired poles were

$-3.9 \pm 12.40j$ and based upon this the closed loop system was analyzed by the following equation.

$$\dot{x} = (A - BG)x$$
$$y = Cx$$

(4)

The gain matrix G can be obtained by the Ackerman method. The block diagram for the pole placement scheme is shown in Figure 3.
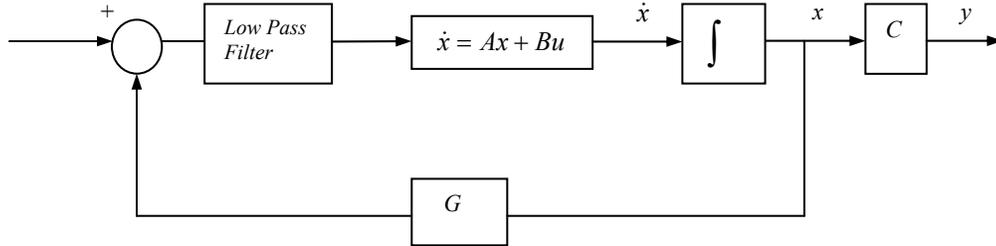

Fig. 3 Block Diagram of Pole Placement Control

3.2 Positive Position Feedback Control

Positive Position Feedback (PPF) control was first proposed by Goh[15] *et al.* for the collocated sensors and actuators. Later on Fanson[15] *et al.* demonstrated PPF control in space structures. The PPF control is applied by feeding the structural position coordinate directly to the compensator, and the product of the compensator and a scalar gain positively back to the structure. PPF offers quick damping for a particular mode provided that the modal characteristics are known. The scalar equations governing the vibration of the structure in a single mode and the PPF controller are given as:

$$\ddot{\xi} + 2\zeta\omega\dot{\xi} + \omega^2\xi = G\omega^2\eta$$

(5)

$$\ddot{\eta} + 2\zeta_c\omega_c\dot{\eta} + \omega_c^2\eta = \omega_c^2\xi$$

(6)

where ξ is a modal coordinate of structure displacement, ζ is the damping ratio of the structure, ω is the natural frequency of the structure, G is the feedback gain, η is the compensator co-ordinate, ζ_c is the damping ratio of the compensator, and ω_c is the natural frequency of the compensator.

The PPF control is illustrated in the block diagram, as shown in Figure 4. In the PPF control, to achieve maximum damping ω_c should be closely matched to the natural frequency ω of the structure.
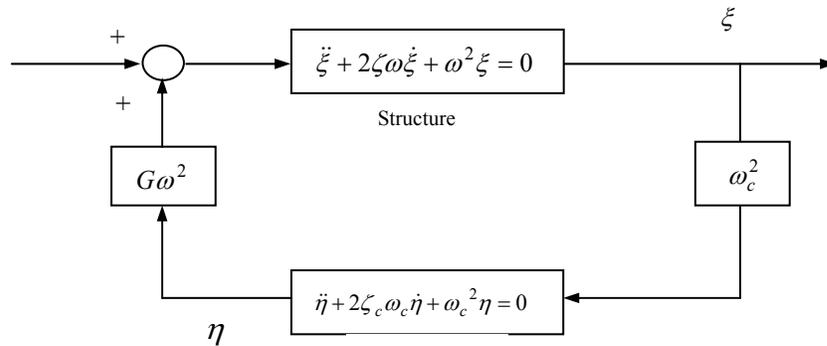

Fig. 4 Block Diagram of PPF Control

3.3 Strain Rate Feedback Control

Strain rate feedback control is implemented by feeding the velocity coordinate to the compensator. The position coordinate of the compensator is then fed back with a negative gain to the structure. When a smart structure is involved using a collocated PZT actuator and sensor, this control is achieved by feeding the derivative of the voltage from the sensor, which is proportional to the strain rate, to the input of the compensator and applying the negative compensator output voltage to the actuator. The scalar equations governing the vibration of the structure in a single mode and the SRF controller are given as:

$$\ddot{\xi} + 2\zeta\omega\dot{\xi} + \omega^2\xi = -G\omega^2\eta \tag{7}$$

$$\ddot{\eta} + 2\zeta_c\omega_c\dot{\eta} + \omega_c^2\eta = \omega_c^2\dot{\xi} \tag{8}$$

The variables above are same as those defined for PPF control. The block diagram for SRF control is shown in Figure 5. In implementing the SRF control the compensator is designed such that the targeted frequencies are below the compensator frequencies. As compared to the PPF, SRF has a much wider active damping frequency region, which gives a designer some flexibility. Selecting a precise compensator frequency for SRF is not as critical as for PPF. As long as the compensator frequency is greater than the structural frequency, a certain amount of damping will be provided.
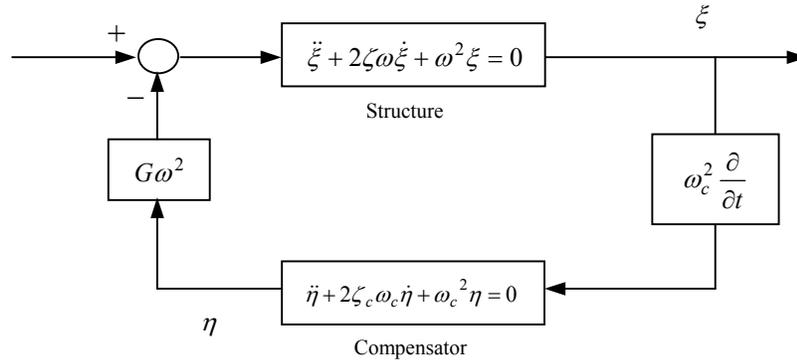

Fig. 5 Block Diagram of SRF Control

3.4 Sliding Mode Control

For the sliding mode control design, we define the following control errors

$$e = y - y^d, \quad \dot{e} = \dot{y} - \dot{y}^d \tag{9}$$

where y and $\dot{y}$ are the strain and strain rate; y^d and $\dot{y}^d$ are the desired strain and strain rate, respectively. Since we consider a vibration control problem, $y^d = 0$ and $\dot{y}^d = 0$. Therefore, $e = y$ and $\dot{e} = \dot{y}$. In this paper, y is directly represented by the fiber Bragg grating sensor output in terms of voltage. Also, defined are auxiliary control variables r and $\dot{r}$ by

$$r = \dot{e} + \lambda e, \quad \dot{r} = \ddot{e} + \lambda\dot{e} \tag{10}$$

where λ is a positive constant. Here, $r = 0$ functions as the sliding surface on which the system is asymptotically stable, i.e., the control error is zero.

The controller is proposed as

$$i = -K_D r - \rho \tanh(ar) \tag{11}$$

where K_D and a are positive constants. The ρ is an upper bound on the uncertainties associated with flexible beam system. In this paper, ρ is also called robust (R) gain. A block diagram of the control system is shown in Figure 6. The functions of each control action in equation (11) are discussed as follows.

The - $K_D r$ term is a linear feedback torque functioning as a Proportional plus Derivative (PD) control. Proportional control is used to decrease steady-state error and increase responsiveness of the actuator. The derivative control is to increase damping and to stabilize the actuator. The -ρtanh(ar) term is a robust compensator and is used to compensate for the uncertainties of the system and to increase control accuracy and stability.
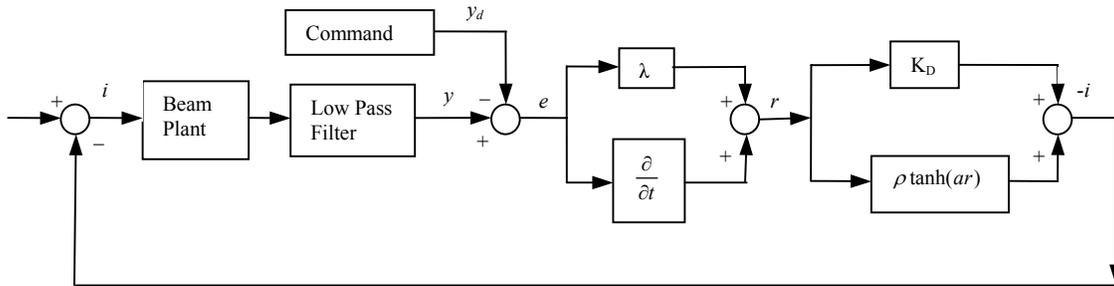
Fig. 6 Block Diagram of Sliding Mode Control

In this control approach, $r=0$ functions as the sliding surface, on which the system is asymptotically stable, i.e., the control error is zero. In order to force the system onto the sliding surface, we employed the so-called smooth robust controller -ρtanh(ar). The robust compensator is continuously differentiable with respect to the control variable r. It generates a smooth control action. Compared with the commonly used bang-bang or saturation robust controllers, the smooth robust controller has advantages in ensuring smooth control input and the stability of the closed-loop system[21]. A detailed comparative study is provided in Song and Mukherjee 1998[27].

The nonlinear nature of the *tanh* function ensures that the compensator functions like a high gain PD controller near $r=0$, which helps to reduce steady state error. The nonlinear nature of the *tanh* function also ensures that and its control action saturates for larger values of r, which avoids overshoot and oscillations. This nonlinear nature of the robust compensator distinguishes itself from a Proportional plus Derivative (PD) controller.

4. EXPERIMENTAL RESULTS OF ACTIVE VIBRATION SUPPRESSION

4.1 Pole Placement Control

The derived transfer function in equation (2) of the system is now used to implement the pole placement design for the desired performance of the system. The plant is discreteized at a sampling frequency of 200 Hz and implemented in real time control system using data acquisition system. The discrete time pole zero plot of the open loop system and the closed loop poles i.e. the desired poles of the system are shown in Figure 7. The systems natural frequency is slightly increased to 13 rad/sec (2.06 Hz) and the poles are moved inside to achieve a higher damping ratio of 0.30.

The open loop test is conducted to view the results in absence of controller. The results of the experimental test and simulated tests are compared. The beam in both cases is actuated using a computerized sinusoidal signal at frequency of 1.63 Hz at 150 Volt coupled with a white noise input for initial 5 seconds. The simulated and experimental results time response is shown in Figure 8. The simulated and experimental results closely match for

the open loop test. With the above results being established and by using the same excitation source, the simulation with the pole placement controller was carried out and the corresponding results are shown in Figure 9. After the initial 5 seconds, the active vibration control is implemented on the aluminum beam to suppress the induced vibration. As it is evident that the vibration that used to take more than 20 seconds to die, now with the use of pole placement control dies down in less than 5 seconds. Next, the real time implementation of the pole placement control was carried. The simulated model was downloaded in data acquisition system and the control scheme was implemented. The experimental result for the controlled and uncontrolled case is shown in Figure 10. The results were close to the simulation results, the vibrations settled down in less than 5 seconds. The Power Spectral Density (PSD) plot for experimental data of 10-15 seconds is shown in Figure 12. A drop of 45 dB as compared to the uncontrolled decibel level is observed during this period of active control. This can also be observed in the simulated frequency responses comparison shown in Figure 11. The simulated frequency response clearly shows the reduction in decibels at the resonance frequency of 1.64 Hz (10 rad/sec). A close correlation is achieved between the simulated and experimental time response results shown in Figure 9 and Figure 10 respectively.
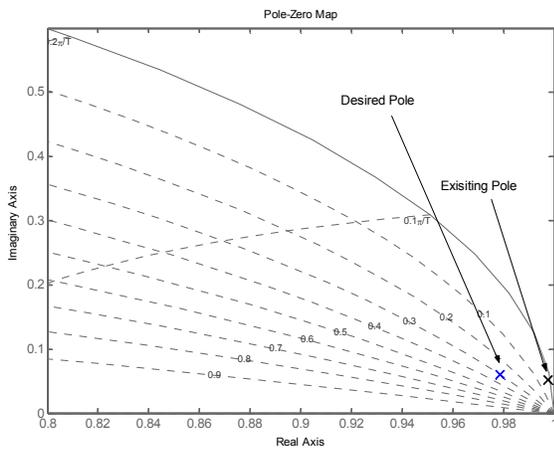

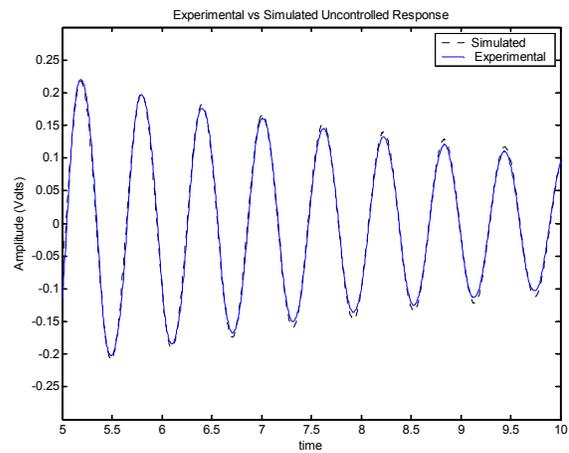Fig. 7 Open (Existing) and Closed loop (Desired) discrete pole locations

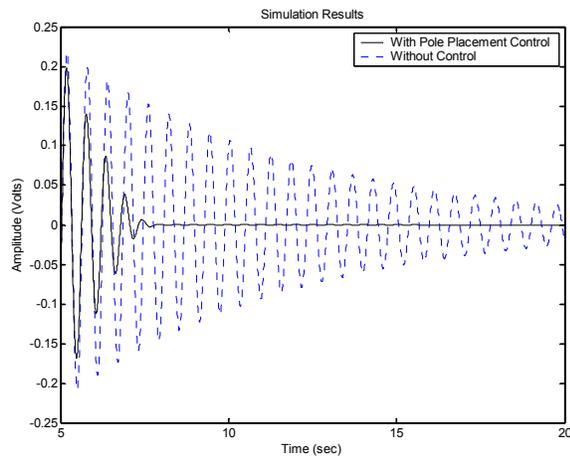Fig. 8 Simulated vs. Experimental open loop time response

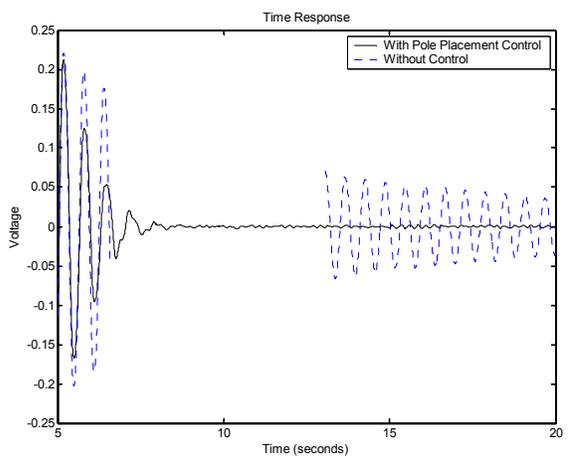Fig. 9 Simulated time response comparison of Pole placement control and without control cases

Fig. 10 Experimental time response comparison of Pole placement control and without control cases

4.2 Positive Position Feedback Control

The positive position feedback control was implemented using the experimental set up described in Section 3. The mode targeted for control was the one at 1.64 Hz. The controller was implemented using in real time control and the data was acquired at sampling frequency of 200 Hz. The PPF controller-damping ratio ζ_c was set to 0.5 and controller frequency ω_c was set at 10.34 rad/sec (1.64 Hz). The controller-damping ratio ζ_c was chosen as a compromise between damping effectiveness and robustness.

As in previous case, to ensure a fair comparison, the beam was excited by a sinusoidal signal with a combination of white noise for the initial 5 seconds in both the uncontrolled and controlled cases. Figure 13 shows comparison of the free vibrations of the beam after the excitation with the corresponding PPF controlled vibrations of the beam. The PPF controlled vibrations of the beam damp out within 5 seconds after excitation. The PSD plot for 10-15 seconds is shown in Figure 14. A drop of 37 dB as compared to the uncontrolled energy level is observed during this period of active control. As compared to pole placement control vibrations take slightly longer time to settle down.

4.3 Strain Rate Feedback Control

The strain rate feedback control (SRF) was implemented real-time on the beam. The mode targeted for real time control was dominant frequency of 1.64 Hz with the data acquired at sampling frequency of 200 Hz. The SRF controller damping ratio ζ_c was set at 0.50, controller frequency ω_c was set at 12.56 rad/sec (2 Hz, which is slightly greater than 1.64 Hz, the targeted mode) and the effectiveness of SRF controller on the beam was tested.

Similar to the other experiments, the beam was excited by a sinusoidal signal and white noise for 5 seconds in both the cases of uncontrolled and controlled vibrations. The SRF controlled time response as compared to free vibrations is depicted in Figure 15. The beam vibrations die within 10 seconds after the excitation signal is stopped. The PSD plot for 10-15 seconds is shown in Figure 16. The SRF control was accompanied with a drop of 35 dB in the energy level of the beam in the period of active control.
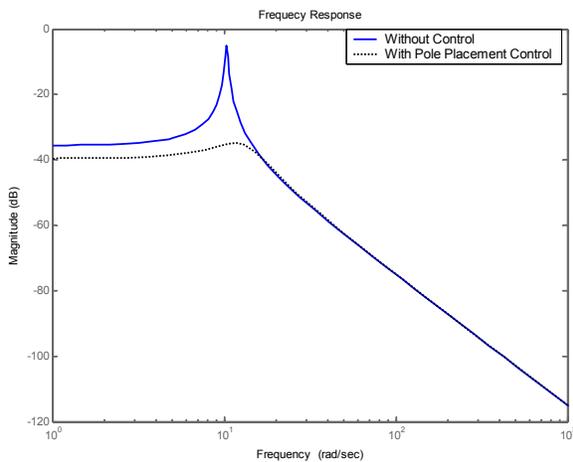

Fig. 11 Simulated Frequency response for the flexible beam for pole placement control and with control cases
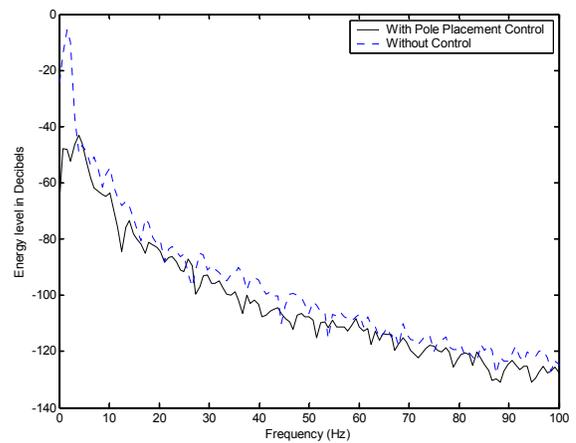
Fig. 12 Power spectral density comparison of Pole placement control and without control cases (10-15 second)
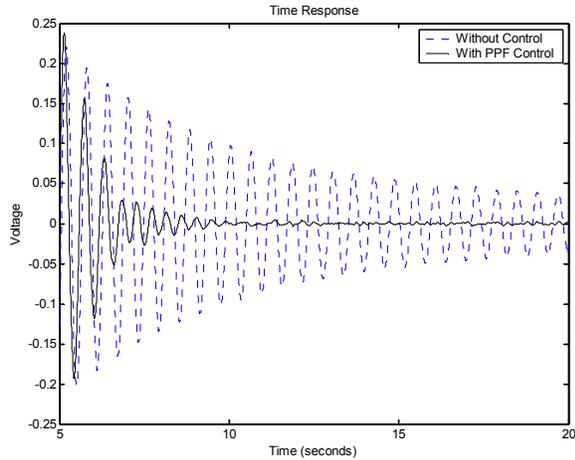
Fig. 13 Experimental time response comparison of PPF control and without control cases
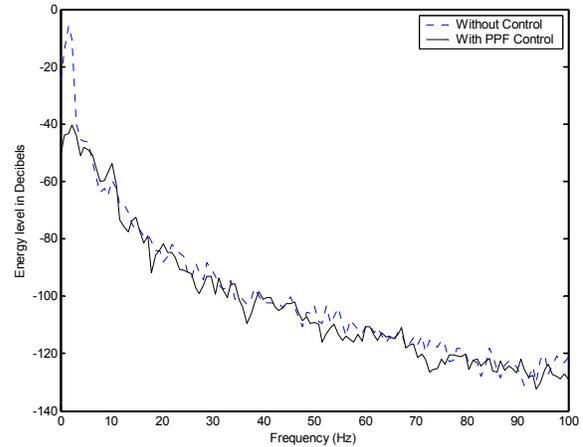

Fig. 14 Power spectral density comparison of PPF control and without control cases (10-15 second)

4.4 Sliding Mode Control

In order to verify the effectiveness of the sliding mode based non linear active vibration control using fiber optics, experimental tests were conducted. The first mode at 1.64 Hz is the target mode for vibration control. The sliding mode control is implemented along with the traditional PD control. Similar to previous tests, the beam is excited by a sinusoidal signal at its first modal frequency combined with a white noise for the initial 5 seconds. After the initial 5 seconds, the active vibration control is implemented on the aluminum beam to suppress the induced vibration. In the first case, a free vibration test is conducted. In this case no active control is involved after the initial 5-second excitation. The data from the fiber optic sensor is acquired and the time response for the controlled and uncontrolled case is plotted in Figure 17. In the controlled case the sliding mode controller, with parameters $K_d = 1$, $\rho = 0.05$, and $\lambda = 15$, is implemented. The comparison of power spectral density plot of the sliding mode control and free vibration is shown in Figures 18. It is clear that the beam vibration is quickly suppressed with the sliding mode control and a 25-dB reduction is achieved.
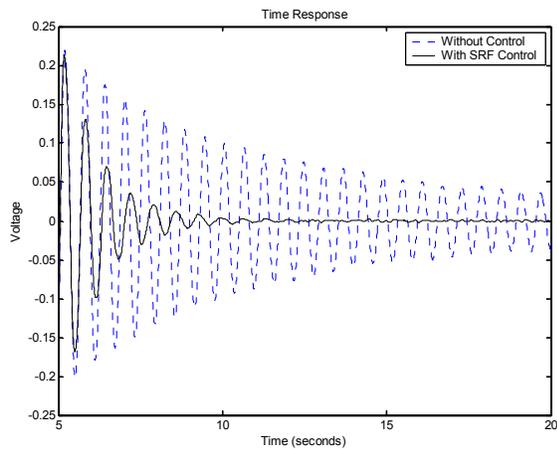

Fig. 15 Experimental time response comparison of SRF control and without control cases
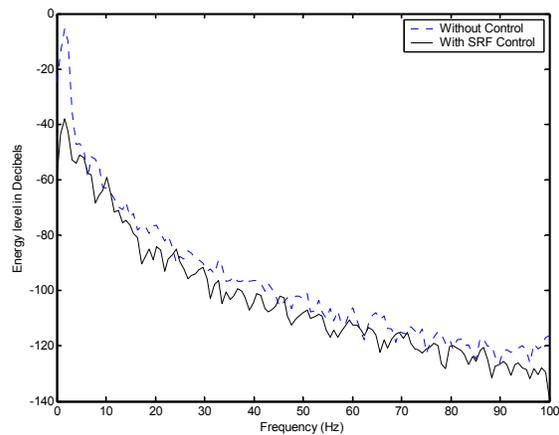

Fig. 16 Power spectral density comparison of SRF control and without control cases (10-15 second)
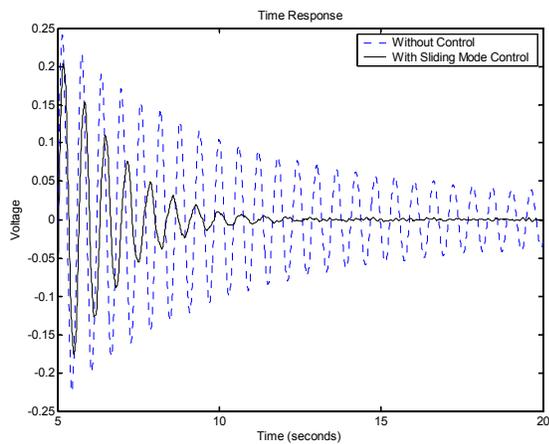
Fig. 17 Experimental time response comparison of sliding mode control and without control cases
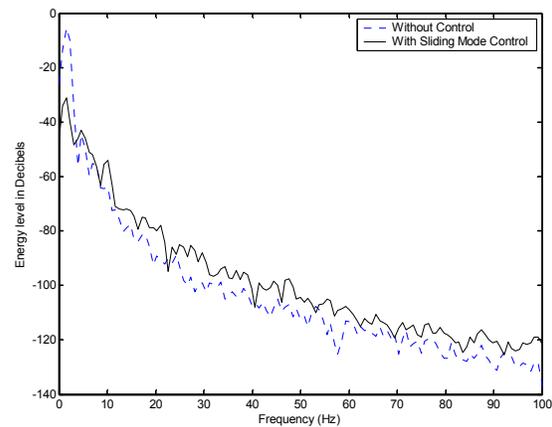
Fig. 18 Power spectral density comparison of Sliding mode control and without control cases (10-15 second)

5. CONCLUSIONS

The experiment results successfully demonstrated the vibration suppression of a flexible beam using the feedback signal from Fiber Bragg Grating sensors for the implementation of pole placement, PPF, SRF and sliding mode control. The single dominant mode vibration suppression was carried out and result was a maximum reduction of 45 dB obtained in pole placement control. The results also confirmed that the FBG sensors can be used for active vibration control for both the linear and non linear control cases. Simulation and experimental results corroborated for the pole placement control case. It was also noticed during experiments that there was some high frequency noise contained in the signal and to eliminate this we required a phase shifter. The phase shifter served a dual purpose of providing amplification to the feedback signal as well as filtering of the high frequency noise content. The justification for the observation of various decibel drops in different experiments and the comparative study is discussed in the paper by Song and Sethi 2003[28]. This experiment also provides an alternative means of measurement for feedback signal. In similar experiments investigators[11, 12, 13, 19, 23] have used piezoelectric patches as sensors. In this paper we proposed and demonstrated FBG's that are rugged, lightweight and immune to electromagnetic interference can be effectively used as sensors for vibration detection and feedback control purposes. A further advantage of these FBG of sensors is they can be multiplexed based on wavelength division multiplexing technique and used to monitor several locations over a long distance using a single light source. Thus our future work will be directed towards using multiple location sensors for vibration control of a smart structure. Finally, we conclude by envisaging that this work will serve as an important milestone for using Fiber Bragg Gratings in vibration suppression experiments.

6. ACKNOWLEDGEMENTS

REFERENCES

[1]   Huston, D. R., Fuhr, P. L., Beliveau, J. G. and Spillman, W. B. Jr., "Structural member vibration measurements using a fiber optic sensor," *J. Sound and Vibration*, **149** (2), pp.348-353, 1991.
[2]   Berkoff, T. A. , Davis, M. A. and Kersey, A. D., "Fiber optic sensors for distributed vibration monitoring," *Proc. SPIE* **2264**, pp. 148-154, 1994.

[3]   Cox, D. E. and Lindner, D. K., "Active Control of vibration suppression in a flexible beam using a modal domain optical fiber sensor," *J. Vibration and Acoustics*, **113**, pp. 369-382, 1991.

[4]   Lindner, D. K., Delos, P. L., Baumann, W. T., "Nonlinear effects of a modal domain fiber optic sensor in a vibration suppressor control loop for a flexible structure," *IEEE South East Conf.* , **1**, pp. 126-129, 1990.

[5]   Juang, P. A. and Wu, M. N., "Active control using a fiber optic interferometric sensor," *Smart Materials and Structures*, **4**, pp. 370-372, 1995.

[6]   Chien, P. Y., Chang, Y.S., Chang, M. W., "Vibration suppression in a flexible structure based on fiber optics Michelson interferometric sensor," *J. of Intelligent Mater. Systems and Struct.*, **7**(1), pp. 65-70, 1996.

[7]   Serdar, K., Mustafa, G., Asmer, H., "Time-delay control of space structures using embedded piezoelectric actuators and fiber optic sensors," *Proc. SPIE* **3041**, pp. 393-405, 1997.

[8]   Beranek, L. L. and Vér, I. L., (Editors), *Noise and Vibration Control Engineering***:** *Principles and Applications***,** Wiley (1992).

[9]   Crawley, E. F. and de Luis, J. "Use of piezoelectric actuators as elements of intelligent structures," *AIAA Journal*, **25**(10), pp. 1373-1385, 1987.

[10]   Crawley, E. F., Luis, J. D., Hagood, N. W. and Anderson, E. H. "Development of piezoelectric technology for applications in control of intelligent structures," *Proc. of the Am. Control Conf.* **88** (3), pp.1890-1896, 1988.

[11]   Crawley, E. F., "Intelligent structures for aerospace: A technology overview and assessment," *AIAA Journal*. **32**(8), pp.1689-1699, 1994.

[12]   Manning, W. J., Plummer, A. R. and Levesley, M. C., "Vibration Control of a flexible beam with integrated actuators and sensors," *Smart Materials and Structures*, **9**, pp. 932-939, 2000.

[13]   Bu, X., Ye, L., Su, Z. and Wang, C., "Active control of a flexible smart beam using a system identification technique based on ARMAX," *Smart Materials and Structures,* **12**, pp. 845-850, 2003.

[14]   Scott, R. G., Brown, M. D. and Levesley, M., "Pole placement control of a smart vibrating beam," *8th Int'l. Congress on Sound and Vibration*, Hong Kong, pp. 387-39, 2001.

[15]   Goh, C. J. and Caughey, T. K., "On the stability problem caused by finite actuator dynamics in the collocated control of large space structure," *Int'l. J. of Control,* **41**(3), pp. 787-802, 1985.

[16]   Fanson, J. L. and Caughey, T. K., "Positive position feedback control for large space structures," *Am. Inst. Aeronaut. Astronaut. J*., **28**(4), pp. 717-724, 1990.

[17]   Agrawal, B. N. and Bang, H., "Adaptive structure for large precision antennas," *45th Congress of the Int'l Astronautical Federation (Jerusalem, Israel)*, Oct. 1994.

[18]   Baz, A. and Poh, S., "Optimal vibration control with modal positive position feedback," *Optimal Control Applications and Methods*, **17**, pp. 141-149, 1996.

[19]   Friswell, M. I. and Inman, D. J., "The relationship between positive position feedback and output feedback controllers," *Smart Materials and Structures*, **8**, pp. 285-291, 1999.

[20]   Song, G., Schmidt, S. P. and Agrawal, B. N., "Active vibration suppression of a flexible structure using smart material and modular control patch," *Proc. Inst. Mech. Engrs,* **214**(G), pp. 217-229, 2000.

[21]   Newman, S. M., "Active damping control of a flexible space structure using piezoelectric sensors and actuators," *Masters Thesis, U.S. Naval Postgraduate School*, December 1992.

[22]   Cai, L. and Song, G., "Joint stick-slip friction compensation of robot manipulators by using smooth robust controllers," *J. Robotic Systems*, **11**(6), pp. 451-470, 1994.

[23]   Melz, G., Morey, W.W., and Glenn, W.H., "Formation of Bragg gratings in optical fibers by a transverse holographic method*," Opt. Lett.,* **14**, pp. 833, 1989.

[24]   Melle, S. et al, "A Bragg grating-tuned fiber laser strain sensor system," *Phot. Tech. Lett.,* **5**, pp. 263-5, 1993.

[25]   Kersey, A. D., Berkoff, T. A., and Morey, W. W., "Fiber-optic Bragg grating strain sensor with drift-compensated high-resolution interferometric wavelength-shift detection," *Opt. Lett.,* Jan 1993.

[26]   Davis, M. A. and Kersey, A. D., "Application of a fiber Fourier transform spectrometer to the detection of wavelength-encoded signals from Bragg grating sensors*," IEEE J. Lightwave Technology,* **13**, 1289, 1995.

[27]   Song, G. and Mukherjee, R., "A comparative study of Conventional Nonsmooth Time-Invariant and Smooth Time-Varying Robust Compensators," *IEEE Trans. Control Systems Technology*, **6**(4), pp. 571-576 1998.

[28]   Song, G. and Sethi, V., "Comparative study of active control of a large composite I-beam," *Int'l J. of Acoustics and Vibration*, **8**(4), pp. 231-238, 2003.

[29]   National Aeronautics and Space Administration/IFOS, "Combining Sense and Intelligence for Smarter Structures", *NASA Spinoff – Fortieth Anniversary Technology Utilization Program* (2002).

[30]   www.ifos.com; http://www.ifos.com/products.html.